International Journal of Advanced Technology in Engineering and Science
Vol. No.5, Issue No. 05, May 2017
www.ijates.com
ijates
ISSN 2348 - 7550

ASSESSMENT OF STRAIN AND STRESS – BASED FORMABILITY DIAGRAMS OF INCONEL 600 HEMISPHERICAL CUPS DRAWN BY SINGLE POINT INCREMENTAL FORMING PROCESS USING ABAQUS

[1]ShashankChagalamarri, G. Devendar[2], A. Chennakesava Reddy[3]

[1]PG Student, Department of Mechanical Engineering, JNT University, Hyderabad (India)

[2]Research Scholar, Department of Mechanical Engineering, JNT University, Hyderabad (India)

[3]Professor, Department of Mechanical Engineering, JNT University, Hyderabad (India)

ABSTRACT

T*he present project work was aimed atassessment of the formability of Inconel 600alloy to manufacturehemispherical cups using single point incremental forming (SPIF) process. The finite element analysis has been carried out to model the single point incremental forming process using ABAQUS software code. The process variables of SPIF were sheet thickness, step depth, tool radius and coefficient of friction. The process variables have been optimized using Taguchi techniques. The major process variables influencing the SPIF of hemispherical cups were tool step depth andcoefficient of friction.*

KEYWORDS: INCONEL 600ALLOY, HEMISPHERICAL CUP, SINGLE POINT INCREMENTAL FORMING, FINITE ELEMENT ANALYSIS, STEP DEPTH, TOOL RADIUS, SHEET THICKNESS, COEFFICIENT OF FRICTION.

I. INTRODUCTION

The use of die block and stiffpunch in the classical deep drawing process does not permit the production of complex shapes especially for the automotive industry. A need for the forming process has emerged to fabricate parts of complex shapes without using dies or punches. In consideration of that, a single point incremental forming (SPIF) process is innovated in recent years. This is a die-less forming processespecially useful to small-lot production for automobile, aerospace andbiomedical industries. During continuous research on SPIF process, a variety of cup shapes such as such as conical [1-4], pyramidal cups [5-7], elliptical cups [8], parabolic cups [9], hyperbolic cups [10] and hemispherical cups [11] have been fabricated. SPIF process has been employed for manufacturing of ankle support [12].Formability of incremental forming process was analyzed by different researchers [13, 14]. The numerical simulations were carried out by variousresearchers for the analysis of SPIF process [15, 16]. The numerical results have been validated with the grid-based experimental results for several materials [17-22].Inconel 600 is a nickel-chromium alloy used for applications that require corrosion and high

temperature resistance. The nickel content in Inconel 600 gives excellent resistance to chlorine stresscorrosion cracking and also provides exceptional resistance to alkaline solutions.Its chromium content gives Inconel 600 resistance to sulfur compounds and various oxidizing environments.

In the present work, the numerical simulation was intended todetermine the strain and stress formability diagrams of hemispherical cups using SPIF process. For this purpose, the design of experiments was executed as per Taguchi technique. The formability was evaluated using finite element analysis software code namely ABAQUS.

II. MATERIAL AND METHODS

In the present work, Inconel600 was used to fabricate hemispherical cups. The chemical composition of Inconel600 is given in Table 1. The levels chosen for the controllable process parameters are summarized in Table 2. Each of the process parameters was chosen at three levels. The orthogonal array (Table 3), L9 was preferred to carry out experimental and finite element analysis (FEA) using ABAQUS software code.

Table 1: Chemical composition of Inconel600

Element	Ni+Co	Cr	Fe	C	Mn	Cu	Si	S
%wt.	72.4	15.9	8.2	1.49	1.0	0.5	0.5	0.01

The sheet and tool geometry were modeled as deformable and analytical rigid bodies, respectively, using ABAQUS. They were assembled as frictional contact bodies. The fixed boundary conditions were given to all four edges of the sheet (figure 1(a)). The sheet material was meshed with S4R shell elements as shown in figure 1(b) [24].The boundary conditions for tool were x, y, z linear movements and rotation about the axis of tool. True stress-true strain experimental data were loaded in the tabular form as material properties. The tool path geometry was generated using CAM software [25] was imported to the ABAQUS as shown in figure 1. The elastic-plastic deformation analysis was carried out for the equivalent stress, strain and strain rates and thickness variation.

Table 1: Process parameters and levels

Factor	Symbol	Level–1	Level–2	Level–3
Sheet thickness, mm	A	1.0	1.2	1.5
Step depth, mm	B	0.50	0.75	1.00
Tool radius, mm	C	4.0	5.0	6.0
Coefficient of friction	D	0.05	0.10	0.15

Table 3: Orthogonal Array (L9) and control parameters

Treat No.	A	B	C	D
1	1	1	1	1
2	1	2	2	2
3	1	3	3	3
4	2	1	2	3

5	2	2	3	1
6	2	3	1	2
7	3	1	3	2
8	3	2	1	3
9	3	3	2	1

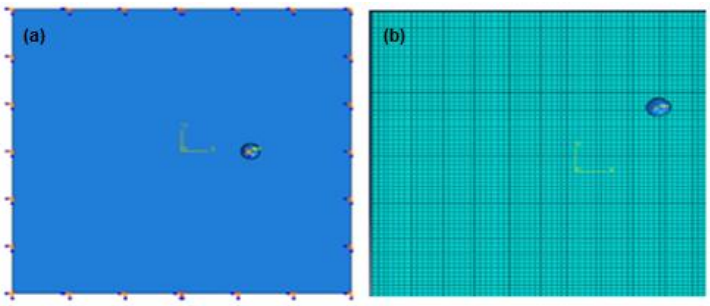

Figure 1. Modelling (a) and discretization (b) of Ni201 sheet.

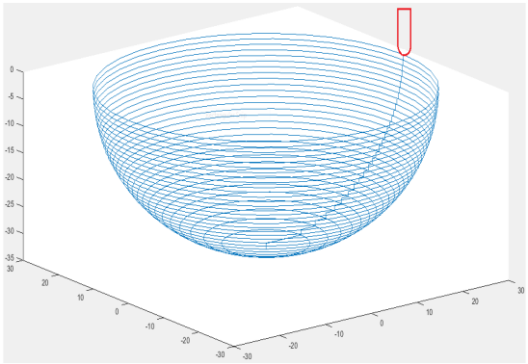

Figure 2: Tool path generation.

III. RESULTS AND DISCUSSION

The controllable process variables were sheet thickness, tool radius, tool step depth and coefficient of friction. In the present work, the significance of process variables should have at least 90% of confidence.

3.1 Influence of process variables on von Mises stress

Table 4 gives the ANOVA (analysis of variation) summary of von Mises stress data. The insignificant process variables were pooled to error. The step depth of the tool contributes only 68.33% of total variation in the von Mises stress.

Table 4: ANOVA summary of the von Mises stress.

Source	Sum 1	Sum 2	Sum 3	SS	v	V	F	P
A	2184.88	2231.87	2184.36	496.10	0	-	-	-
B	2163.21	2138.79	2299.11	4974.04	2	2487.02	6.40	68.33

C	2166.71	2226.19	2208.20	620.29	0	-		-
D	2193.78	2210.21	2197.11	50.30	0	-	-	-
e-pooled	-	-	-	2333.39	6	388.90		31.67
T	8708.59	8807.06	8888.78	6140.73	8	-	-	100

Note: *SS is the sum of square, v is the degrees of freedom, V is the variance, P is the percentage of contribution and T is the sum squares due to total variation.*

Figure 3 presents the influence of step depth of the tool on the von Mises stress induced in Inconel 600 alloy. For tool step depth of 0.5 mm and 0.75 mm, the von Mises stress is not affected, but it increases drastically for step depth of 1.0 mm. The von Mises increases with an increase in the equivalent plastic strain up to 0.5 irrespective of sheet thickness and later on it decreases as shown in figure 5.

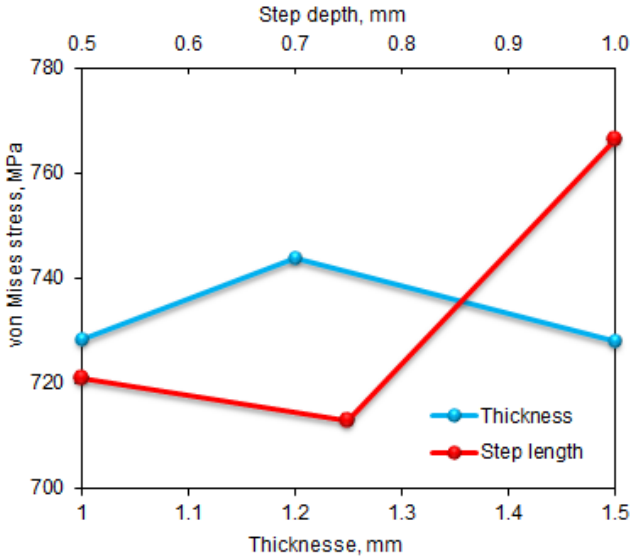

Figure 3: Influence of tool step depth on von Mises stress.

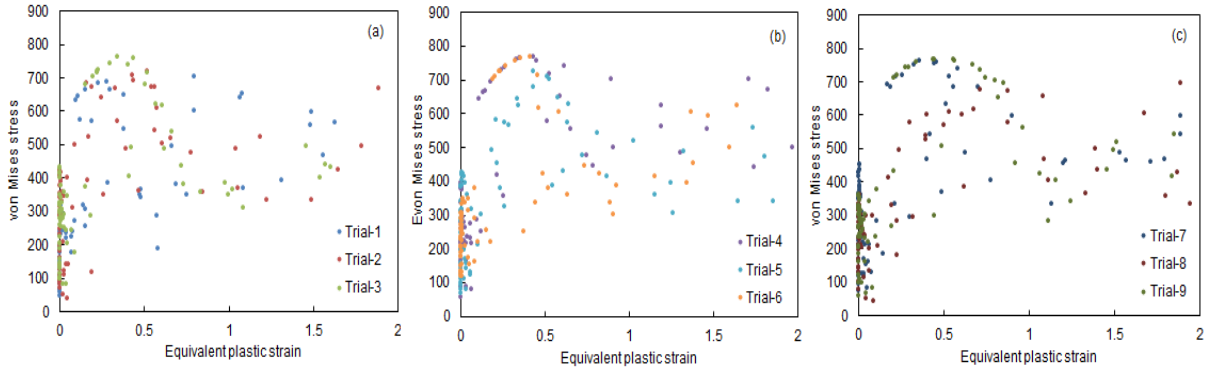

Figure 4: ***Effect of equivalent plastic strain on von Mises stress: (a) 1.0 mm, (b) 1.2 mm and (c) 1.5 mm sheet thickness.***

The equivalent plastic strain reaches its maximum value at half portion of the hemispherical cup wall from the flange and it starts decreasing along another half portion till the bottom of the cup reached as shown in figure 5. But, the von Mises stress increases from the flange to the bottom of cup, of course with fluctuation. The von Mises stresses induced in the cups are 743 MPa, 729 MPa, 769 MPa, 769 MPa, 734 MPa, 769 MPa, 768 MPa, 695 MPa, and 768 MPa, respectively for trials 1, 2, 3, 4, 5, 6, 7, 8, and 9 as shown in figure 6. The trials 3, 4, 6, 7 and 9 have the same von Mises stress values. The least stress induced is 695 MPa in the trial 8. It is also detected that the maximum stress (red in color) is induced in bottom and on side walls of the cup. In all the hemispherical cups, the von Mises stress is minimum in the flange area. The ultimate tensile strength of Inconel 600 alloy is 824 MPa which is not exceeded in all the cases. The von Mises stress is exceeded the yield strength (580 MPa) of Inconel 600 alloy in all the cases. The von Mises stress was steeply down at bottom (the last portion to be formed) of the hemispherical cup due to sufficient plastic deformation experienced by Inconel 600 alloy as shown in figure 5(b).

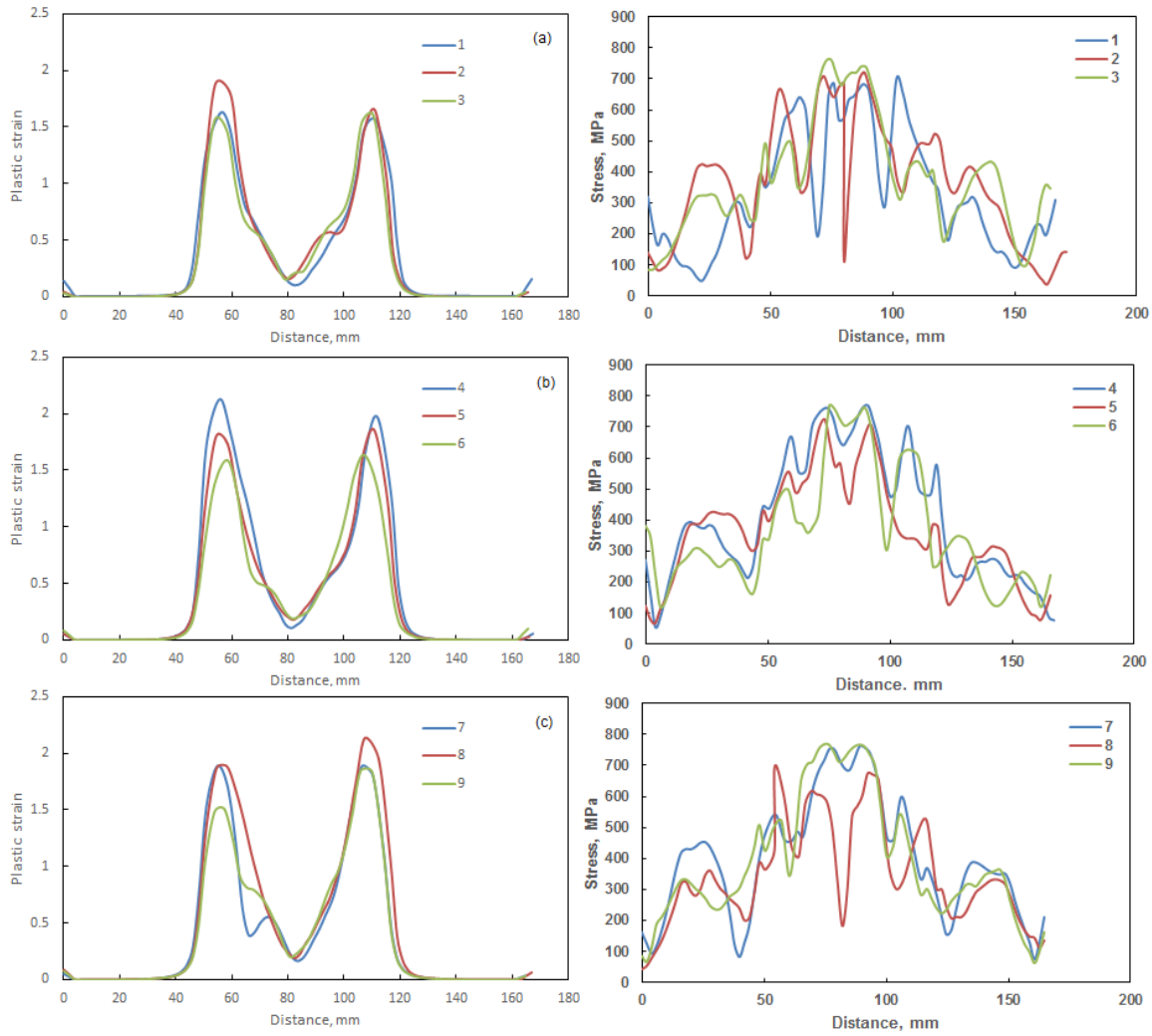

Figure 5: Variation of equivalent plastic strain and von Mises stress along a path from flange to bottom of cup: (a) 1.0

mm, (b) 1.2 mm and (c) 1.5 mm sheet thickness.

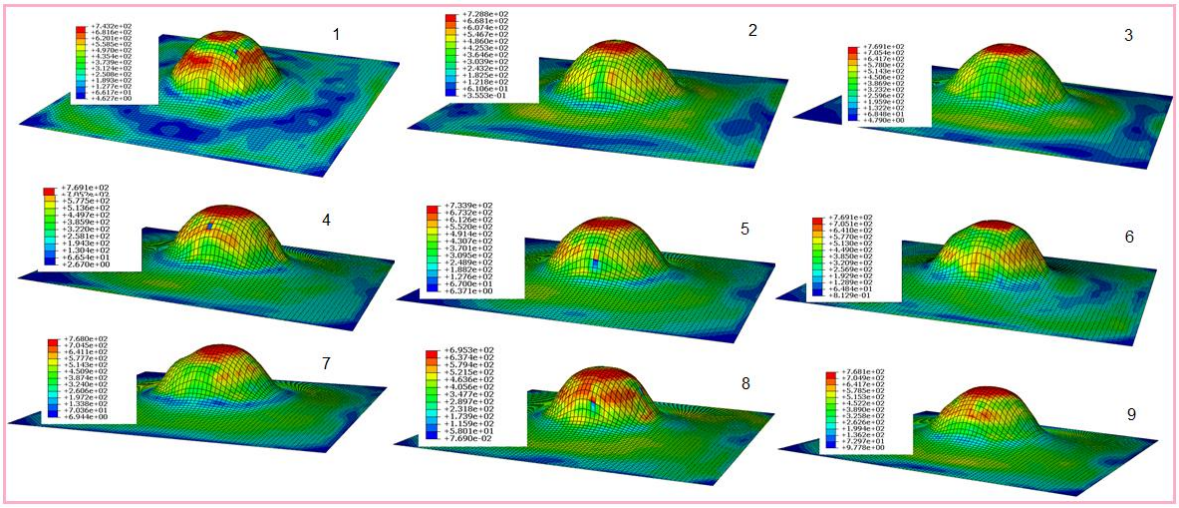

Figure 6: The von Mises stress induced in the hemispherical cups of all trial runs.

3.2 Influence of parameters on thickness reduction

The ANOVA summary of the thickness reduction is given in Table 5. The thickness reduction during the cup drawing is only dependent on the coefficient of friction only. The other process variables have negligible influence on the thickness reduction of the hemispherical cup.The thickness reduction is found to be high for the friction coefficients of 0.05 and 0.15 except for 0.10 as shown in figure 7(a). The thickness strain distribution along the component and the effect of coefficient of friction have been studied for the superplastic forming of Ti-Al-4V alloy in [26]. It has been found that a lower friction coefficient results in a better thickness strain distribution along the component.The necking has occurred at the middle of the cup wall as seen in figure 7(b). This phenomenon (blue in color) can be seen in the raster images shown in figure 8. In evaluation of local thinning during cup drawing of steel using isotropic criteria [27], it has been concluded that the strain is maximum at the thinner sections. The maximum local thinning ranges from 52% to 58% for the hemispherical cups drawn using SPIF.

Table 5: ANOVA summary of the thickness reduction

Source	Sum 1	Sum 2	Sum 3	SS	v	V	F	P
A	165.16	167.26	167.21	0.96	0	-	-	0.00
B	168.79	167.78	163.06	6.22	0	-	-	0.00
C	168.52	166.47	164.64	2.52	0	-	-	0.00
D	171.31	158.35	169.97	33.87	2	16.94	5.24	62.91
e	-	-	-	19.39	6	3.23	-	37.09
T	673.78	659.86	664.88	43.57	8	-	-	100.00

International Journal of Advanced Technology in Engineering and Science
Vol. No.5, Issue No. 05, May 2017
www.ijates.com
ijates
ISSN 2348 - 7550

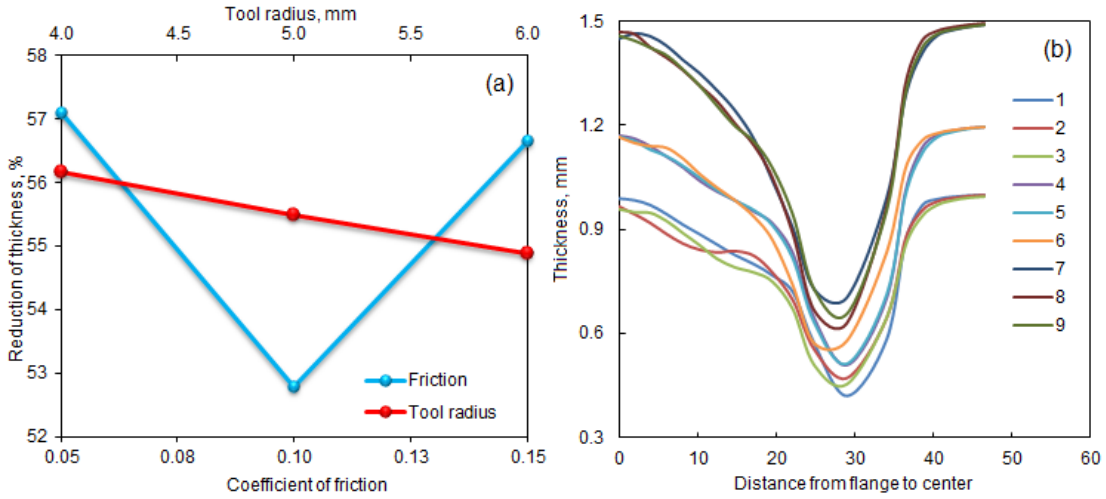

Figure 7: Effect of friction coefficient on thickness reduction: (a) ANOVA results and (b) thickness reduction along a path from flange to center of the cup.

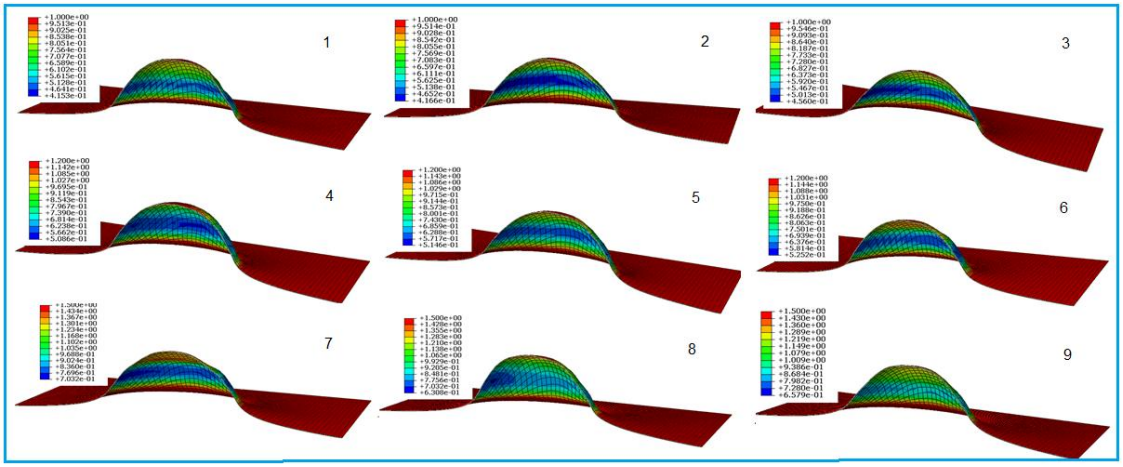

Figure 8. The reduction in thickness of the parabolic cups for all trial runs.

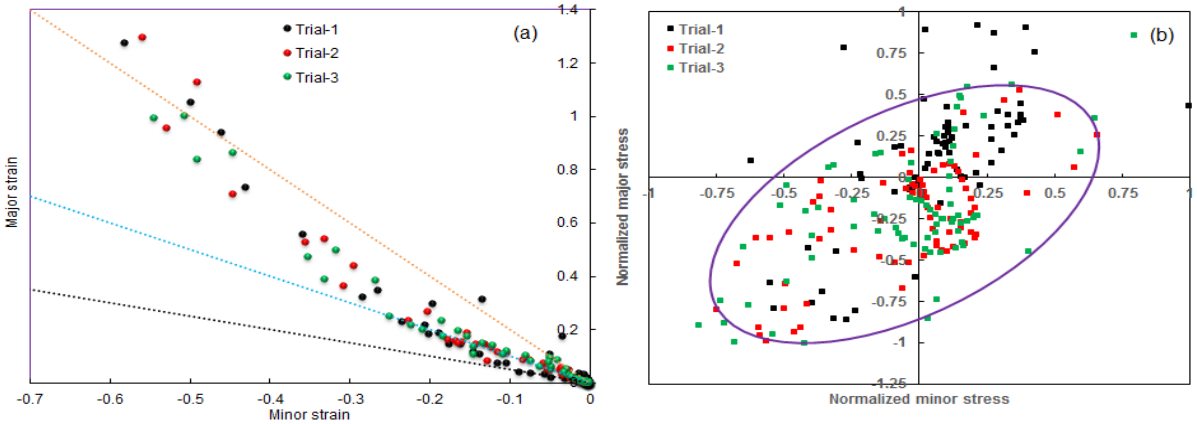

Figure 9: Forming limit diagrams for trials 1, 2, 3: Strain-based, and (b) Stress-based.

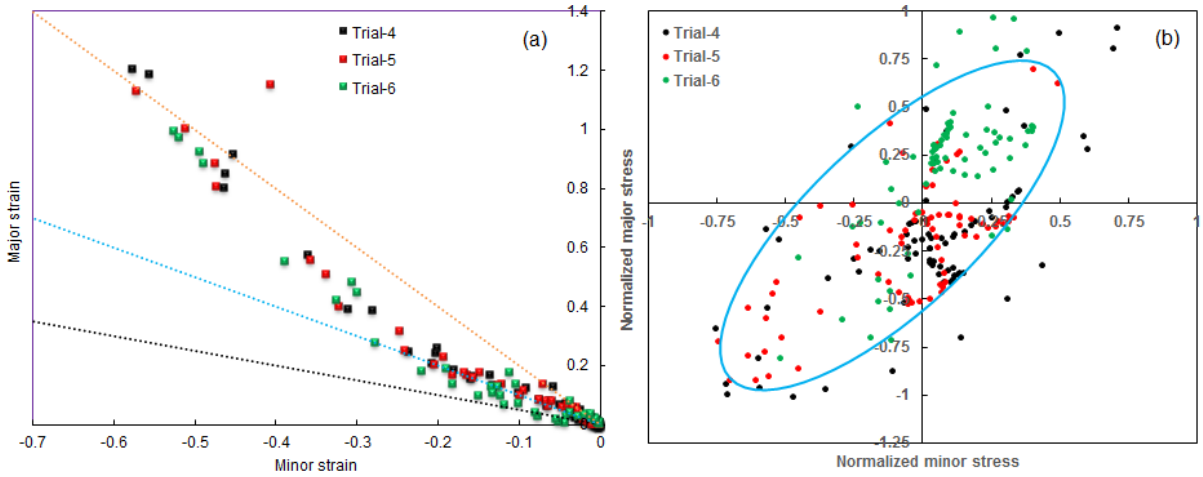

Figure 10: Forming limit diagrams for trials 4, 5, 6: Strain-based, and (b) Stress-based.

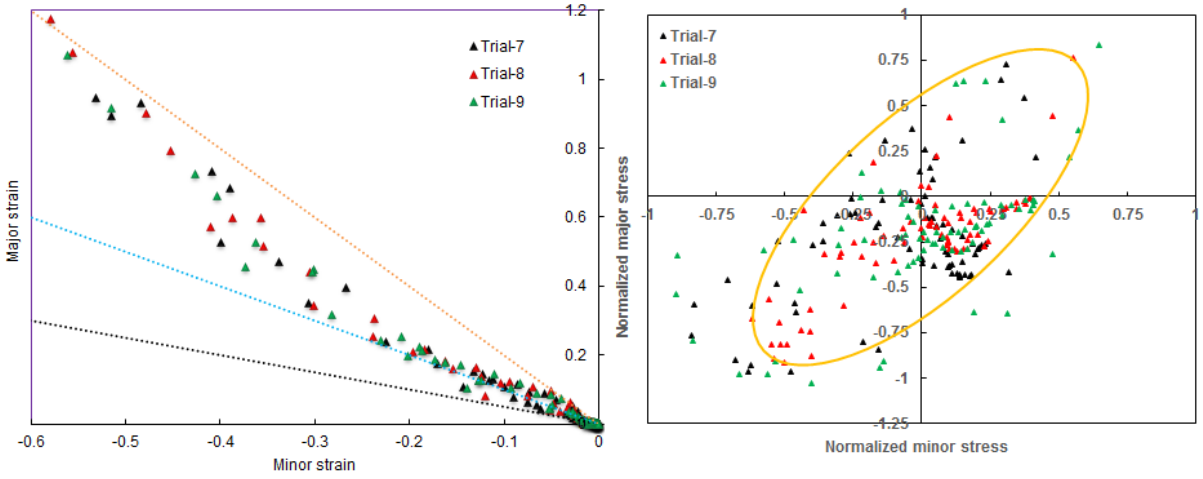

Figure 11: Forming limit diagrams for trials 7, 8, 9: Strain-based, and (b) Stress-based.

3.3 Formability of hemispherical cups

The strain-based formability diagrams of the cups are shown in figures9(a), 10(a) and 11(a). Uni-axial tension is exceedingly subjugated during the formation of hemispherical cups. The stress-based formability diagrams of the cups are shown in figures 9(b), 10(b) and 11(b). The major and minor stresses were normalized using the ultimate tensile strength (824 MPa) of Inconel 600. For the trial 2 (figure 9(b)), trial 5 (figure 10(b)), and trial 8 (figure 11(b)), the normalized stresses are less than absolute unity. The lowest von Mises stress is 695 MPa for the trail 8. The conditions for the trial 9 given Table 6 are considered to be the optimum process variables for the hemispherical cups drawn using SPIF.

Table 6. Optimum process parameters for parabolic cups

Trial No.	Sheet thickness (A), mm	Step depth (B), mm	Tool radius (c), mm	Coefficient of friction (D)
8	1.5 (level 3)	0.75 (level 2)	4.0 (level 1)	0.15 level 3)

IV. CONCLUSIONS

The major SPIF process parameters which influence the formability of hemispherical cups of Inconel 600alloy were tool step depth and coefficient of friction. In all the trials of SPIF process, the von Mises stresses induced in the Inconel 600 alloy sheet did not exceed its ultimate tensile strength. Major thinning of the sheet material has occurred at middle portion of the hemispherical cup walls.

REFERENCES

[1] T. Santhosh Kumar, V. Srija, A. Ravi Teja, A. C. Reddy, Influence of Process Parameters of Single Point Incremental Deep Drawing Process for Truncated Pyramidal Cups from 304 Stainless Steel Using FEA, International Journal of Scientific & Engineering Research, 2016, vol. 7, no. 6, pp. 100-105.

[2] V. Srija, A. C. Reddy, Single Point Incremental Forming of AA1050-H18 Alloy Frustum of Cone Cups, International Journal of Science and Research, 2016, vol. 5, no. 6, pp. 1138-1143.

[3] T. Santhosh Kumar, A. C. Reddy, Single Point Incremental Forming and Significance of Its Process Parameters on Formability of Conical Cups Fabricated from AA1100-H18 Alloy, International Journal of Engineering Inventions, 2016, vol. 5, no. 6, pp. 10-18.

[4] A. Raviteja, A. C. Reddy, Implication of Process Parameters of Single Point Incremental Forming for Conical Frustum Cups from Aa 1070 Using FEA, International Journal of Research in Engineering and Technology, 2016, vol. 5, no. 6, pp. 124-129.

[5] T. Santhosh Kumar. A. C. Reddy, Finite Element Analysis of Formability of Pyramid-Al Cups Fabricated from AA1100-H18 Alloy, International Journal of Science and Research, 2016, vol. 5, no. 6, pp. 1172-1177.

[6] A. Raviteja, A. C. Reddy, Finite Element Analysis of Single Point Incremental Deep Drawing Process for Truncated Pyramidal Cups from AA1070 Alloy, International Journal of Innovative Science, Engineering & Technology, 2016, vol. 3, no. 6, pp. 263-268.

[7] V. Srija, A. C. Reddy, Numerical Simulation of Truncated Pyramidal Cups of AA1050-H18 Alloy Fabricated by Single Point Incremental Forming, International Journal of Engineering Sciences & Research Technology, 2016, vol. 5, no. 6, pp. 741-749.

[8] B. Navya Sri, A. C. Reddy, Formability of Elliptical SS304 Cups in Single Point Incremental Forming Process by Finite Element Method, International Journal of Research in Engineering & Technology, 2016, vol. 4, no. 11, pp. 9-16.

[9] K. Sai Santosh Kumar, A. C. Reddy, Die Less Single Point Incremental Forming Process of AA6082 Sheet Metal to Draw Parabolic Cups Using ABAQUS, International Journal of Advanced Technology in Engineering and Science, 2016, vol. 4, no. 11, pp. 127-134.

[10] T. Manohar Reddy, A. C. Reddy, Numerical Investigations on The Single Point Incremental Forming of 60-40 Brass to Fabricate Hyperbolic Cups, International Journal of Advance Research in Science and Engineering, 2016, vol. 5, no. 11, pp. 161-170.

[11] G. Soujanya, A. C. Reddy, Analysis of Single Point Incremental Forming Process to Fabricate Phosphorous Bronze Hemispherical Cups, International Journal of Innovative Science, Engineering & Technology, 2016, vol. 3, no. 11, pp. 139-144.

[12] Ambrogio, G., De Napoli, L., 2005. Application of Incremental Forming process for high customised medical product manufacturing. Journal of Materials ProcessingTechnology 162-163 (2005) 156-162.

[13] Y.H. Kim, J.J. Park, Effect of process parameters on formability in incremental forming of sheet metal, Journal ofMaterials Processing Technology 130-131 (2002) 42-46.

[14] J. Kopac, Z. Kampus, Incremental sheet metal forming on CNC milling machine-tool, Journal of Materials ProcessingTechnology 162-163 (2005) 622-628.

[15] L. Fratini., Ambrogio, G., Lorenzo, D. R., Filice, L., Micari, F., Influence of mechanical properties of the sheet material on formability in single point incremental forming, Annals of CIRP, 2004, vol. 53, pp. 207-210.

[16] H. Iseki, K. Kato, S. Sakamoto, Forming limit of flexible and incremental sheet metal bulging with a spherical roller, Proceedings of the Fourth International Conference on Technology of Plasticity, Advanced Technology of Plasticity, 1993.

[17] C. R. Alavala, Fem Analysis of Single Point Incremental Forming Process and Validation with Grid-Based Experimental Deformation Analysis, International Journal of Mechanical Engineering, 2016, vol. 5, no. 5, pp. 1-6.

[18] C. R. Alavala, Validation of Single Point Incremental Forming Process for Deep Drawn Pyramidal Cups Using Experimental Grid-Based Deformation, International Journal of Engineering Sciences & Research Technology, 2016, vol. 5, no. 8, pp. 481-488.

[19] A. C. Reddy, Numerical and Experimental Investigation of Single Point Incremental Forming Process for Phosphorus Bronze Hemispherical Cups, International Journal of Scientific & Engineering Research, 2017, vol. 8, no. 1, pp. 957-963.

[20] A. C. Reddy, Evaluation of Single Point Incremental Forming Process for Parabolic AA6082 Cups, International Journal of Scientific & Engineering Research, 2017, vol. 8, no. 1, pp. 964-970.

[21] A. C. Reddy, Experimental and Numerical Studies on Formability of Stainless Steel 304 In Incremental Sheet Metal Forming of Elliptical Cups, International Journal of Scientific & Engineering Research, 2017, vol. 8, no. 1, pp. 971-976.

[22] A. C. Reddy, Pilot Studies on Single Point Incremental Forming Process for Hyperbolic Brass Cups, International Journal of Scientific & Engineering Research, 2017, vol. 8, no. 1, pp. 977-982.

[23] J. Jeswiet, D. Young, M. Ham, Non-Traditional Forming Limit Diagrams for Incremental Forming. Advanced Materials Research, 2005, vol. 6-8, pp. 409-416.

[24] C.R. Alavala, “Finite Element Methods: Basic Concepts and Applications,” PHI Learning Pvt. Ltd., New Delhi, 2008.

[25] C.R. Alavala, “CAD/CAM: Concepts and Applications,” PHI Learning Pvt. Ltd., New Delhi, 2008.

[26] A. C. Reddy, "Finite element analysis of reverse superplastic blow forming of Ti-Al-4V alloy for optimized control of thickness variation using ABAQUS," Journal of Manufacturing Engineering, 2006, vol. 1, no.1, pp.06-09.

[27] A. C. Reddy, "Evaluation of local thinning during cup drawing of gas cylinder steel using isotropic criteria," International Journal of Engineering and Materials Sciences, 2012, vol. 5, no. 2, pp.71-76.